Front. Med. 2025, 19(6): 1086−1098
https://doi.org/10.1007/s11684-025-1172-0

RESEARCH ARTICLE

Yinqiao powder effectively alleviates acute lung injury via regulating cGAS-STING signaling pathway

Hui Li[1,2,3,4,*], Jincai Wen[3,4,5,*], Yuanyuan Cui[1,*], Sichen Wang[3,4], Wei Shi[3,4], Huijie Yang[3,4], Li Lin[3,4], Yuanyuan Guo[3,4], Xiaohe Xiao (✉)[3,4], Junling Cao (✉)[6], Zhaofang Bai (✉)[3,4], Ping Zhang (✉)[1]

[1]Department of Pharmacy, Medical Supplies Center of PLA General Hospital, Beijing 100853, China; [2]Beijing Hospital of Traditional Chinese Medicine, Capital Medical University, Beijing 100010, China; [3]Department of Hepatology, The Fifth Medical Center of PLA General Hospital, Beijing 100039, China; [4]China Military Institute of Chinese Materia, The Fifth Medical Center of PLA General Hospital, Beijing 100039, China; [5]School of Pharmacy, Chengdu University of Traditional Chinese Medicine, Chengdu 611137, China; [6]Dongfang Hospital, Beijing University of Chinese Medicine, Beijing 100078, China

Abstract **Acute lung injury (ALI) is a respiratory disease characterized by inflammation. Yinqiao powder (YQP) is a traditional Chinese medicinal compound, extensively used for its heat-clearing and detoxifying effects. It is usually used clinically to treat respiratory diseases, such as pneumonia. However, the exact mechanism by which YQP treats ALI remains unclear. Here, we aimed to explore the therapeutic effects and potential mechanisms of action of YQP in ALI. Activation of the cGAS-STING pathway was modeled by multiple stimuli in bone marrow-derived macrophages (BMDMs), THP-1, and peripheral blood mononuclear cells (PBMCs). Changes in the content of associated proteins were detected by Western blot, while the mRNA levels of type I interferon-related genes and proinflammatory cytokines were detected by qPCR. A DMXAA-induced agonist model was used to verify the effect of YQP on the cGAS-STING pathway *in vivo*, whereas LPS-induced ALI was used to explore the therapeutic effect of YQP. YQP suppressed the activation of the cGAS-STING pathway *in vitro*. YQP showed promising therapeutic effects on DMXAA-induced activation of the cGAS-STING signaling pathway as well as the LPS-induced ALI model in mice. YQP alleviated ALI by inhibiting cGAS-STING pathway activation; meanwhile, YQP may be a new therapeutic approach for cGAS-STING-driven inflammatory diseases.**

Keywords Yinqiao powder; acute lung injury; cGAS-STING signaling pathway; inflammation; TBK1-IRF3

Introduction

Acute lung injury (ALI), a severe respiratory disease, commonly results from pathogenic infections, trauma, burns, and drug reactions—all of which induce a systemic inflammatory reaction that contributes to the development of ALI [1]. In severe cases, it can cause acute respiratory distress syndrome (ARDS), carrying a death rate as high as 50% [2,3]. As a key supportive therapeutic measure, mechanical ventilation is extensively used in the clinical practice [4,5]. Despite significant advancements in ALI therapy, there are no effective drugs for ALI, making it difficult to substantially reduce the death rate and improve patients' quality of life [6]. The prevailing view is that uncontrolled inflammation in the lungs or throughout the body is the main pathogenesis [7–9]. Therefore, finding new therapeutic drugs, especially new treatment methods to control the inflammatory response in ALI, is of crucial importance.

Increasing evidence suggests that the regulation of inflammatory factors by the cyclic GMP-AMP synthase-stimulator of interferon genes (cGAS-STING) signaling pathway is crucial for disease progression [10,11]. Notably, the cGAS-STING pathway plays a central role in the onset and progression of ALI [12,13]. Cellular damage and the release of abnormal DNA may be triggering factors for the activation of the cGAS-STING pathway in multiple diseases. cGAS, a specialized DNA sensor, recognizes double-stranded DNA and catalyzes the formation of 2′3′-cyclic guanosine monophosphate

Received April 22, 2025; accepted August 14, 2025

Correspondence: Ping Zhang, zhp1231@126.com;
Zhaofang Bai, baizf2008@hotmail.com;
Junling Cao, caojunling72@163.com;
Xiaohe Xiao, pharmacy_302@126.com

*These authors contributed equally to this work.

(2′3′-cGAMP), which subsequently binds and activates STING present in the endoplasmic reticulum membrane [14,15]. After dimerization to form a tetramer oligomerization, the activated STING protein undergoes translocation from the endoplasmic reticulum to the Golgi apparatus, where it recruits and phosphorylates TANK binding kinase 1 (TBK1) to form a complex, and the phosphorylated TBK1 in turn phosphorylates STING [16–18]. The activated STING complex recruits and phosphorylates interferon regulatory factor 3 (IRF3) to form a functional STING signalosome, and activated IRF3 undergoes nuclear entry and regulates type I interferon-related genes [19,20]. In turn, activated STING affects the NF-κB pathway by modulating IκB kinase, which then regulates the expression of proinflammatory cytokines [21,22]. Studies have shown that zinc oxide nanoparticles (ZnONPs) inhalation induces ALI in mice and activates cGAS and STING, thereby aggravating the pathological changes in the lungs, oxidative stress, and inflammation. The cGAS inhibitor RU.521 suppressed cGAS-STING pathway activation, reduced oxidative stress and inflammation, and attenuated lung injury in ZnONP-treated mice [23]. Thus, targeting the regulation of the cGAS-STING pathway is an attractive strategy for the treatment of ALI.

In recent years, traditional Chinese medicinal compounds, as an essential part of traditional Chinese medicine (TCM), have shown unique advantages, especially playing an irreplaceable role in the treatment of pulmonary inflammation caused by COVID-19 and improvement of disease prognosis [24–26]. Yinqiao powder (YQP), as a classic TCM compound, has the effects of "cold-pungent diaphoresis" and "heat-clearing and detoxifying" [27]. It is typically used to treat influenza, upper respiratory tract infection, and pneumonia [28–30]. Research has shown that this formula, along with its key components like forsythin, chlorogenic acid, and baicalin, can treat respiratory system diseases by regulating various immune-related signaling pathways [30–32]. For example, YQP promotes autophagy-dependent ROS decrease to inhibit ROS/NLRP3/pyroptosis regulation axis in influenza virus infection [33]. YQP also play a crucial role in anti-influenza virus activity by regulating TLR7/NF-κB signal pathway [34]. More importantly, *Lonicera japonica* Thunb. and *Forsythia suspensa* (Thunb.) Vahl, as the core drug pair of YQP, can alleviate systemic inflammation by inhibiting the cGAS-STING pathway [35]. Based on the anti-inflammatory effect of YQP, further studies on the role of YQP in ALI and its related molecular mechanisms, especially its relationship with the cGAS-STING pathway, are important for the prevention and treatment of ALI.

In this work, we discovered that the YQP effectively suppressed the cGAS-STING pathway in cells derived from both humans and mice, and further research revealed that it effectively inhibited the interaction between TBK1 and IRF3. Notably, YQP has a good ameliorating effect on ALI induced by lipopolysaccharide (LPS), positioning it as a candidate compound for diseases treatment through the cGAS-STING signaling pathway.

Materials and methods

Reagents and antibodies

Drugs and reagents: YQP was obtained from Beijing Tcmages Pharmaceutical Co., Ltd. (Beijing, China). The dose of YQP used in the animal experiments was converted from a clinically equivalent dose (4.68 g/kg) and a double dose (9.36 g/kg). Dulbecco's modified Eagle medium (DMEM, CM10013, Macgene), RPMI-1640 (CM10040, Macgene), fetal bovine serum (FBS, C04001, VivaCell), mouse IL-6 ELISA kits (1210602, DAKEWE), mouse TNF-α ELISA kits (1217202, DAKEWE), protease inhibitor cocktail (C0001, TargetMol), C-176 (HY-112906, MedChemExpress), murine macrophage colony-stimulating factor (M-CSF, HY-P7085, MedChemExpress), 2× RealStar Fast SYBR qPCR Mix (A304-10, GenStar).

The following antibodies were used: anti-IRF3 (phospho Ser396) antibody (GTX86691, GeneTex), anti-IRF3 (phospho S386) antibody (ab76493, abcam), anti-IRF3 polyclonal antibody (11312-1-AP, Proteintech), anti-TMEM173/STING polyclonal antibody (19851-AP, Proteintech), anti-HSP90 polyclonal antibody (13171-1-AP, Proteintech), anti-actin antibody (sc-8432, Santa Cruz Biotechnology), anti-Lamin B1 antibody (sc-374015, Santa Cruz).

Cell culture and preparation

Bone marrow-derived macrophages (BMDMs) used in this study were obtained from C57BL/6J healthy mice, then cultured in DMEM containing 10% FBS, 1% penicillin/streptomycin (P/S), and 50 ng/mL M-CSF. HEK-293T cells were cultured in DMEM containing 10% FBS and 1% P/S. When the density of HEK-293T cells reached 80%–90%, we discarded the old culture medium, washed the cells with PBS, and then added 0.25% trypsin for digestion for 1 min. Digestion was terminated with DMEM, and the cell suspension was centrifuged. The cells were then resuspend and inoculated into the culture dishes at a ratio of 1:3 to complete the passage. THP-1 were kept in RPMI-1640 and induced to differentiate into macrophages by 100 nmol/L PMA stimulation for 4–5 h. Human peripheral blood mononuclear cells (PBMCs)

were cultured in RPMI-1640. All cells were maintained at a constant temperature of 37 °C and 5% CO_2.

Cell viability assay

BMDMs (1×10^6/mL) and THP-1 (1.5×10^6/mL) cells were seeded in 96-well cell culture plates and treated with YQP (0, 0.125, 0.25, 0.5, 1, and 2 mg/mL) for 12 h on the following day. Absorbance (450 nm) was measured using a microplate reader, according to the instructions of CCK-8.

STING oligomerization assay

BMDMs (1.1×10^6/mL) and THP-1 (1.5×10^6/mL) cells were cultured in 12-well culture plates for 18 h, treated with YQP or vehicle (Opti-MEM) for 1 h, and then stimulated with 2′3′-cGAMP for 30 min. The cells were then lysed with lysis buffer for a duration of 15 min. The cell lysate was collected and centrifuged at 7500 *g* for 10 min at 4 °C, and divided into two portions, which were then added to loading buffer with or without SDS. The portion without SDS was loaded into the gel without SDS, run for 1 h, and then immunoblotted with the anti-STING antibody. The SDS-containing fraction was loaded into a gel containing SDS and then immunoblotted with the anti-HSP90 antibody.

Immunoprecipitation assay

HEK-293T cells (5.5×10^6/mL) were seeded in 6-well culture plates for 18 h, after which they were transfected with HA-tagged or Flag-tagged plasmids per well for 24 h, followed by exposure of the cells to YQP or Opti-MEM for 6 h. Then, the cells were lysed with lysis buffer. The cell supernatant was collected at 4 °C for 30 min and centrifuged at 4 °C, 750 *g* for 5 min. A portion of the cell supernatant was aspirated and added to 1× loading buffer as input, and the remaining supernatant was incubated with anti-Flag-M2 magnetic beads for 5 h at 4 °C. The samples were centrifuged and washed twice with lysate buffer, followed by the addition of loading buffer as an IP, and the expression of the corresponding antibodies was detected by immunoblotting.

Animals

C57BL/6J (7-week-old, weighing 20 ± 2 g) mice in these experiments were obtained from SPF Biotechnology Co., Ltd. (Beijing, China). They were bred under specific conditions (temperature 22–26 °C; humidity 55%–65%).

For DMXAA-induced agonist experiments *in vivo*, female C57BL/6J mice were acclimatized for 1 week and then pretreated with YQP (9.36 g/kg) or saline for 5 days. The mice were anesthetized 4 h after intraperitoneal injection of DMXAA (25 mg/kg). Peritoneal lavage fluid was collected by rinsing the abdominal cavity of mice with pre-cooled PBS, and serum was obtained. The peritoneal lavage fluid was centrifuged, and then cells in peritoneal lavage fluid were collected and subsequently extracted for total RNA. The expression levels of IFN-β, TNF-α, IL-6, and CXCL10 were detected using ELISA or qPCR.

For LPS-induced ALI experiments, male C57BL/6J mice were acclimatized and fed for 1 week. The mice were given saline or different concentrations of YQP (4.68 g/kg or 9.36 g/kg) by gavage for 5 days. Then, they were anesthetized and then given a drop of LPS (4 mg/kg) through the trachea. After 12 h, the mice were anesthetized. Bronchoalveolar lavage fluid (BALF) was collected by rising the lungs with pre-cooled PBS, and lung tissues were collected. The levels of the inflammatory cytokines IL-6 and TNF-α in BALF were measured using ELISA kits. Lung tissues were used for hematoxylin-eosin (HE) staining to detect pathological tissue changes, and was homogenized and lysed with Trizol reagent. Total RNA was extracted to detect the mRNA levels of the type I interferon and proinflammatory cytokine genes.

cDNA preparation and qPCR assay

Cell or tissue samples were lysed with Trizol reagent and RNA was extracted following previous literature [36]. Total RNA was reverse-transcribed into cDNA. qPCR was then processed using the SYBR Green qPCR Master Mix. The expression levels of related genes were calculated using β-actin as a reference.

Western blot

Following the methodology delineated in a precedent study, cellular proteins were extracted and dissolved in loading buffer [37]. The lysates were dispersed by gel electrophoresis, transferred to polyvinylidene fluoride (PVDF) membranes, and sealed for 1 h, then incubated with primary and secondary antibodies. The target bands were detected using an enhanced chemiluminescence detection reagent. HSP90 or actin was used as the controls.

Statistical analysis

GraphPad Prism 8.0 was utilized for charting and statistical analysis. Comparisons between the two groups were performed using unpaired Student's *t*-test, and statistical analysis among multiple groups was performed

using one-way ANOVA with Dunnett's post hoc test. All data were presented as mean ± standard error of the mean (SEM). Differences were defined as statistically significant at $P < 0.05$.

Results

YQP inhibits the activation of cGAS-STING signaling pathway

First, cell viability was tested using the CCK-8 assay. The results showed that the concentration of YQP (0–2 mg/mL) didn't inhibit the viability of BMDMs and THP-1 cells at 12 h (Fig. 1A and 1B). We selected a safe concentration range of YQP for further experiments.

Next, we investigated the impact of YQP on the cGAS-STING pathway. The effect of YQP on Interferon-stimulatory DNA (ISD)-induced cGAS-STING pathway activation was assessed. BMDMs were pretreated with YQP for 1 h and then activated with ISD. It showed that YQP markedly suppressed the levels of p-IRF3 and p-STING in BMDMs (Fig. 1C). Meanwhile, we detected the function of YQP on the expression of downstream factors activated by ISD using qPCR assay. This indicated that YQP reduced the mRNA levels of IFN-β, TNF-α, IL-6, CXCL10, and ISG15, in a concentration (Fig. 1D–1H). Similarly, we transfected THP-1 cells with exogenous ISD to validate the impact of YQP on the cGAS-STING pathway. It obtained that YQP reversed the induction of THP-1 cells by ISD and significantly decreased the expression of type I interferon and inflammatory factors (Fig. 1I–1N).

YQP suppresses the cGAS-STING signaling pathway mediated by multiple stimuli

Based on these results, we used multiple agonists to activate the cGAS-STING pathway, aiming to explore if YQP exerts a wide-ranging inhibitory influence on this pathway. DMXAA, a STING agonist, is known to activate the cGAS-STING pathway in mice, but has no effect in human [38]. We performed relevant experiments on three cell types: BMDMs, THP-1 cells, and human PBMCs. The results revealed that YQP inhibited the phosphorylation of IRF3 and STING induced by ISD, 2′3′-cGAMP, diABZI, and DMXAA in BMDMs (Fig. 2A). Moreover, there was a notable decrease in the mRNA expression of IFN-β, TNF-α, and IL-6 following YQP treatment (Fig. 2D–2F). Subsequently, 2′3′-cGAMP and ISD were used to activate the cGAS-STING signaling pathway to detect the effects of YQP on THP-1 cells and PBMCs. The results indicated that YQP inhibited the activation of STING and IRF3 by both agonists (Fig. 2B), and decreased the mRNA levels of IFN-β, TNF-α, and IL-6 (Fig. 2G–2I). The results validated in PBMCs were consistent with those obtained in THP-1 cells (Fig. 2C, 2J–2L). In summary, these results suggest that YQP suppresses the cGAS-STING pathway induced by various stimuli.

YQP reduces nuclear translocation of IRF3 in BMDMs and THP-1

Nuclear translocation of IRF3 is an important downstream signaling event during cGAS-STING activation [16]. When STING is activated, it attracts TBK1 to form a complex, driving IRF3 to dimerize and undergo nuclear translocation, whereas STING activates the NF-κB pathway [39]. The effect of YQP on IRF3 nuclear translocation following 2′3′-cGAMP stimulation was examined by isolating the cytoplasm and nucleus in our study. BMDMs and THP-1 cells were pretreated with vehicle or YQP, followed by 2′3′-cGAMP to stimulate the cells. This indicated that the cGAS-STING pathway was activated by 2′3′-cGAMP, and IRF3 exhibited a tendency for nuclear translocation; however, nuclear entry was significantly reduced by treatment with YQP (Fig. 3A and 3B). This indicated that YQP plays a role in inhibiting the nuclear entry of IRF3 in this process.

YQP inhibited TBK1-IRF3 interaction, but had no impact on STING oligomerization and the interaction of STING-TBK1 or STING-IRF3

STING oligomerization is a vital upstream signaling event: after receiving a signal delivered by 2′3′-cGAMP, STING undergoes oligomerization and then undergoes translocation from the endoplasmic reticulum to the Golgi apparatus [40]. Therefore, we investigated the effects of YQP on STING oligomerization. This demonstrated that YQP did not affect STING oligomerization under 2′3′-cGAMP stimulation, suggesting that the stage of YQP action is located after STING oligomerization (Fig. 3C and 3D).

Research has revealed that the activation of STING recruits and activates TBK1 while forming the STING-TBK1 complex and recruiting IRF3, resulting in its dimerization and nuclear translocation [18,41]. Hence, we investigated the effect of YQP on this important process by transfecting exogenous. HEK-293T cells were expressed with HA-tagged plasmids (HA-STING and HA-IRF3) or flag-tagged plasmids (Flag-IRF3 and Flag-TBK1) followed by treatment with YQP. Immunoprecipitation experiments were performed to detect the interactions between STING, IRF3, and TBK1. The results showed that administration of YQP affected TBK1-IRF3 binding, but had no impact on STING-TBK1 or STING-IRF3 binding, suggesting that YQP exerts its inhibitory effect by blocking the binding of IRF3 to TBK1 (Fig. 3E–3G).

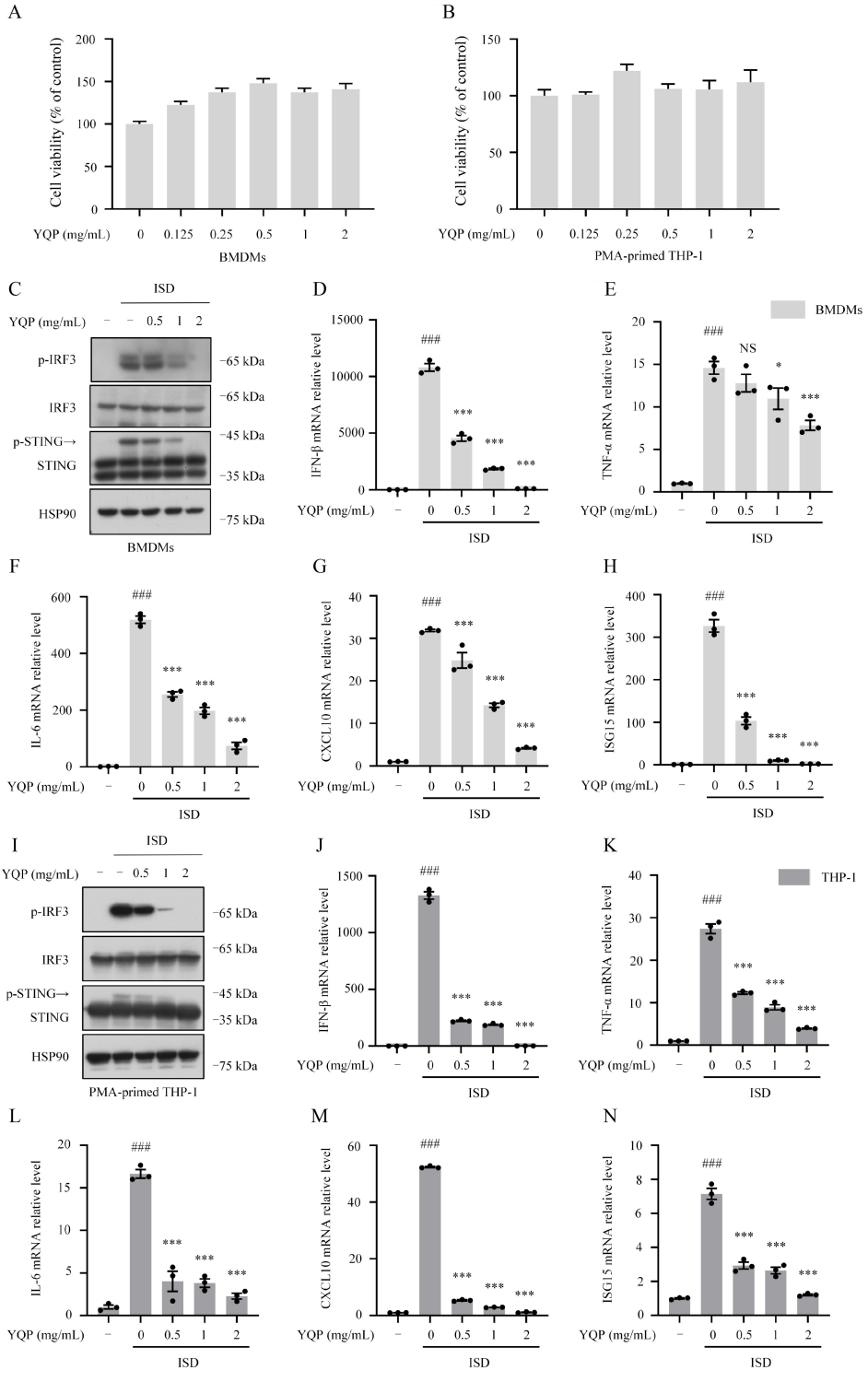

Fig. 1 YQP inhibits the activation of cGAS-STING signaling pathway. (A, B) BMDMs or PMA-primed THP-1 cells were treated with YQP for 12 h. The cell viability was determined by CCK-8 assay. (C) BMDMs was treated with YQP (0.5, 1, and 2 mg/mL) for 1 h, and then transfected for ISD stimulation for 2 h. Western blot was used to detect the expression of p-IRF3, p-STING, STING, IRF3, and HSP90. (D–H) BMDMs were treated with YQP (0.5, 1, and 2 mg/mL) for 1 h, and then transfected for ISD stimulation for 4 h. The expression of IFN-β, TNF-α, IL-6, CXCL10, and ISG15 was detected by qPCR. (I) PMA-primed THP-1 cells were treated with YQP (0.5, 1, and 2 mg/mL) for 1 h, and then transfected for ISD stimulation for 2 h. Western blot was used to detect the expression of p-IRF3, p-STING, STING, IRF3, and HSP90. (J–N) PMA-primed THP-1 cells were treated with YQP (0.5, 1, and 2 mg/mL) for 1 h, and then transfected for ISD stimulation for 4 h. The expression of IFN-β, TNF-α, IL-6, CXCL10, and ISG15 was detected by qPCR. All data are expressed as mean ± SEM. Statistical differences were analyzed by one-way ANOVA and Dunnett's post hoc test. $^{###}P < 0.001$ vs. control group; $^{*}P < 0.05$, $^{***}P < 0.001$ vs. model group; NS, non-significant differences.

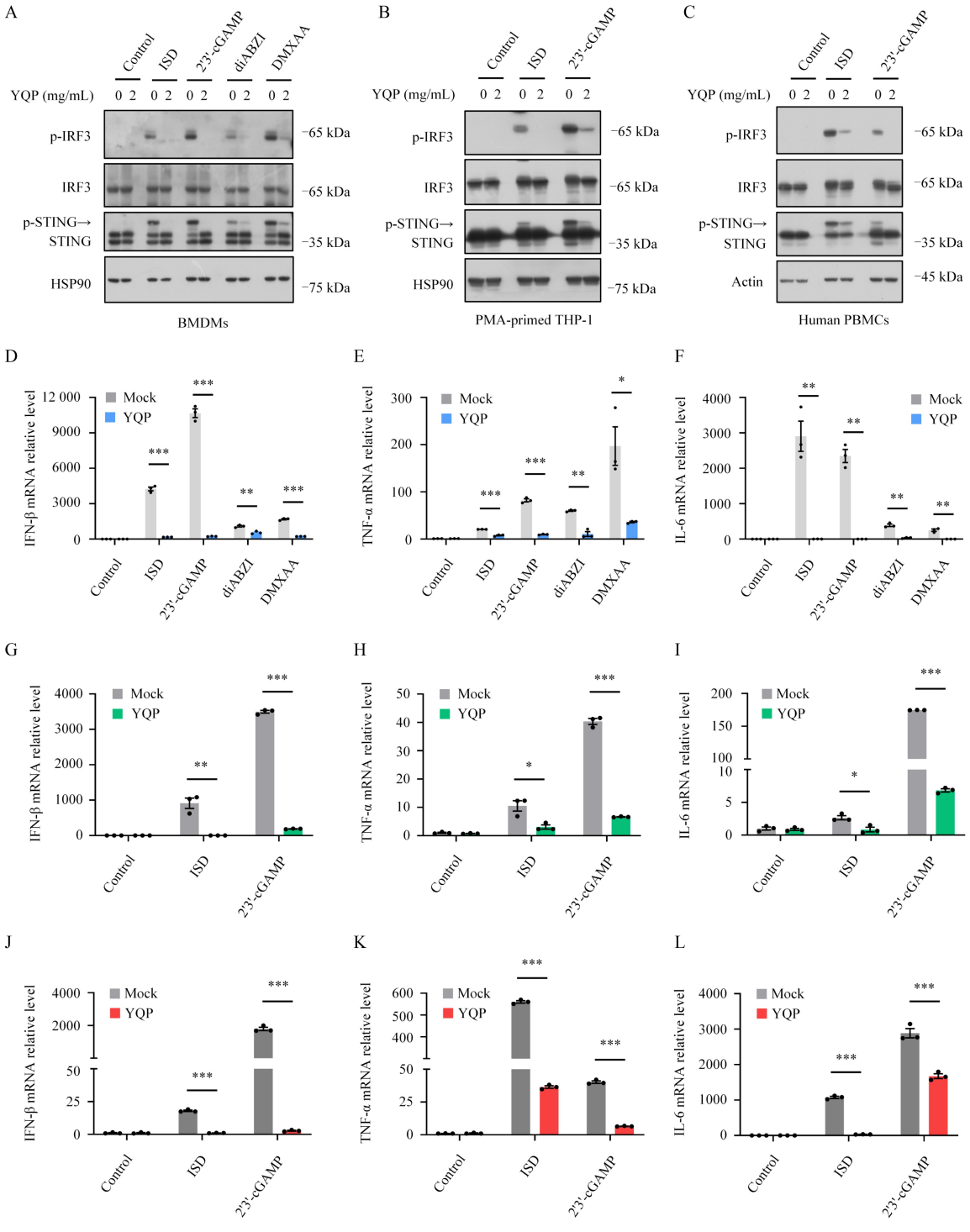

Fig. 2 YQP suppresses the cGAS-STING signaling pathway mediated by multiple stimuli. (A) BMDMs were treated with YQP (2 mg/mL) for 1 h, followed by ISD, 2′3′-cGAMP, diABZI, and DMXAA for 2 h. The expression levels of p-IRF3, p-STING, STING, IRF3, and HSP90 were detected by Western blot. (B, C) PMA-primed THP-1 or human PBMCs were treated with YQP (2 mg/mL) for 1 h, followed by ISD, 2′3′-cGAMP for 2 h. The expression levels of p-IRF3, p-STING, STING, IRF3, and HSP90 (or actin) were detected by Western blot. (D–F) BMDMs was treated with YQP (2 mg/mL) for 1 h, followed by ISD and 2′3′-cGAMP for 4 h. The expression levels of IFN-β, TNF-α, and IL-6 were detected by qPCR. (G–I) PMA-primed THP-1 and (J–L) human PBMCs were treated with YQP (2 mg/mL) for 1 h, followed by ISD and 2′3′-cGAMP for 4 h. The expression of IFN-β, TNF-α, and IL-6 was detected by qPCR. All data are expressed as mean ± SEM. Statistical differences were analyzed by unpaired *t*-test. $^{*}P < 0.05$, $^{**}P < 0.01$, $^{***}P < 0.001$.

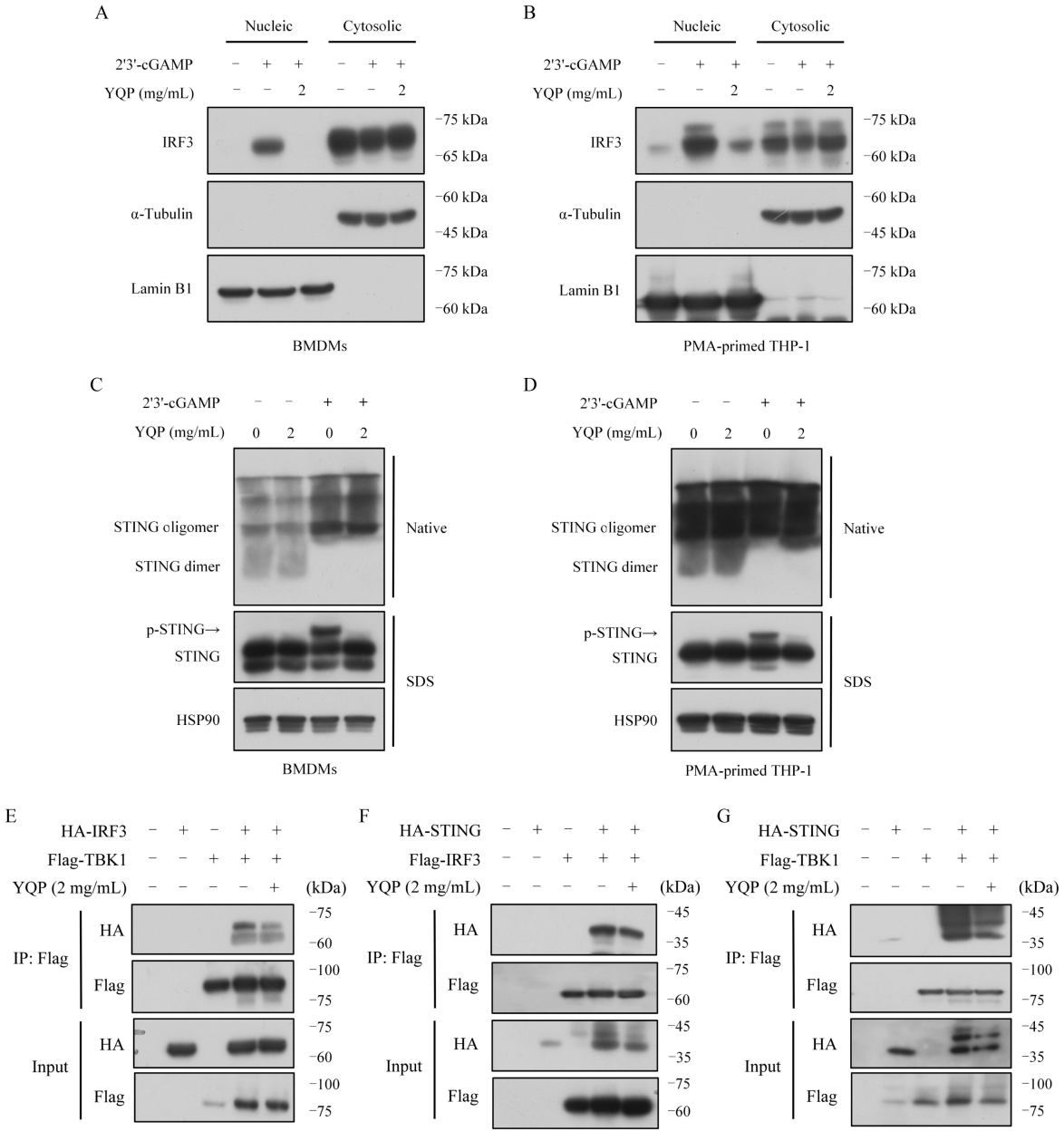

Fig. 3 YQP targets STING signalsome formation without affecting STING oligomerization. (A, B) BMDMs or PMA-primed THP-1 cells were treated with YQP (2 mg/mL) for 1 h and then stimulated with 2′3′-cGAMP for 2 h. The proteins of cytoplasm and nucleus were separated using kits and detected by Western blot. (C, D) BMDMs or PMA-primed THP-1 cells were treated with YQP (2 mg/mL) for 1 h and then transfected with 2′3′-cGAMP for 2 h. Phosphorylation and oligomerization of STING were detected by Western blot. (E–G) HA-tagged plasmids (HA-STING, HA-IRF3) or flag-tagged plasmids (Flag-IRF3, Flag-TBK1) were transfected into HEK-293T. Then cells were treated with YQP (2 mg/mL). Immunoprecipitation was performed with anti-Flag M2 affinity gel beads and Western blot analysis showed results.

YQP effectively suppresses DMXAA-induced activation of cGAS-STING pathway *in vivo*

The above results suggest that YQP effectively suppressed the cGAS-STING pathway *in vitro*. To further verify whether YQP achieves the inhibitory impact *in vivo*, we established the cGAS-STING activation model by injecting the STING agonist. DMXAA is an immune system stimulant that can activate the STING pathway to induce the release of type I interferons and pro-inflammatory cytokines. It is commonly used in research on immune and inflammatory-related mechanisms [36]. Mice were given vehicle or YQP for 5 days, followed by peritoneal injection of DMXAA for modeling. The results showed that the expression levels of IFN-β, TNF-α, and IL-6 were markedly reduced after YQP treatment in the serum and lavage fluid (Fig. 4A–4F). Moreover, the mRNA levels of IFN-β,

TNF-α, and CXCL10 in the peritoneal lavage fluid cells were reduced (Fig. 4G–4I). Overall, the results indicated that YQP effectively inhibited the activation of the cGAS-STING pathway *in vivo*.

YQP has therapeutic effect on LPS-induced ALI

It is reported that the cGAS-STING pathway is associated with initiation and maintenance of several inflammatory diseases [42]. Targeted suppression of the cGAS-STING pathway is a vital strategy for attenuating lung inflammation and injury. LPS, a crucial constituent of the outer membrane of Gram-negative bacteria, is a common pathogenic factor in various inflammatory diseases including ALI [43,44]. Tracheal drip LPS has been extensively utilized to study the pathological effects of ALI, with the advantage that this method does not lead to a systemic inflammatory response or multi-organ failure [45]. C-176, an exclusive STING inhibitor, effectively attenuates ALI in mice [46]. In our research, we chose the LPS-induced ALI model and tested YQP efficacy with C-176 as a positive drug. The experimental process is illustrated in Fig. 5A.

Pulmonary edema and alveolar enlargement are common clinical symptoms of ALI [47]. The wet/dry

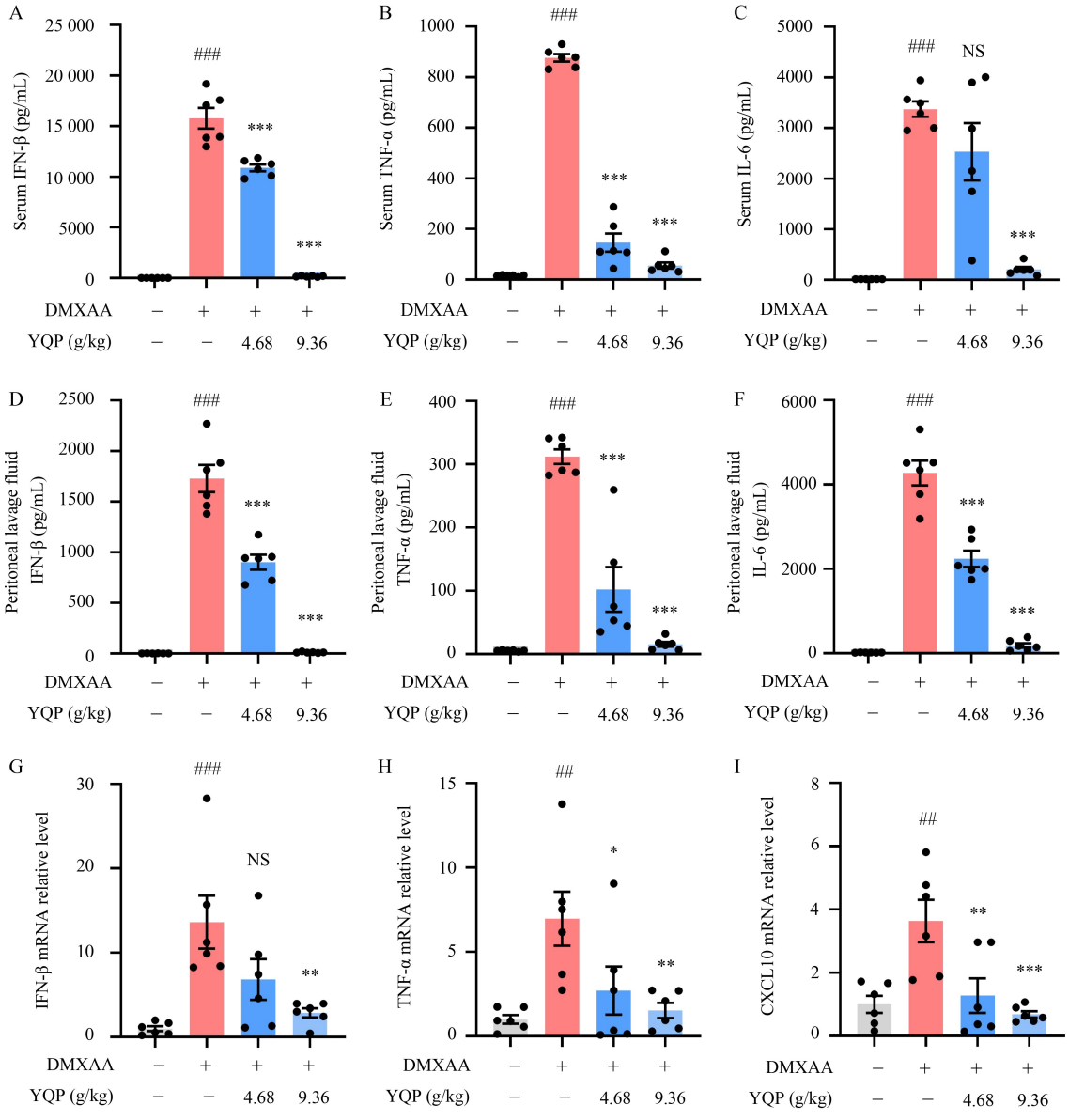

Fig. 4 YQP effectively suppresses DMXAA-induced activation of cGAS-STING pathway *in vivo*. (A–C) The expression levels of IFN-β, TNF-α, and IL-6 in serum were determined by ELISA. (D–F) The expression levels of IFN-β, TNF-α, and IL-6 in peritoneal lavage fluid were determined by ELISA. (G–I) The expression levels of IFN-β, TNF-α, and CXCL10 in cells from peritoneal lavage fluid were detected by qPCR. All data are expressed as mean ± SEM. Statistical differences were analyzed by one-way ANOVA and Dunnett's post hoc test. $^{\#\#}P < 0.01$,$^{\#\#\#}P < 0.001$ vs. control group; $^{*}P < 0.05$, $^{**}P < 0.01$, $^{***}P < 0.001$ vs. model group; NS, non-significant differences.

(W/D) weight ratio of the lung tissue was determined to explore the effect of YQP on pulmonary edema. The experimental findings suggested that, in comparison with the control group, tracheal drip LPS caused a higher W/D ratio. Meanwhile, the treatment with YQP visibly alleviated lung edema (Fig. 5B). Then, the pathological

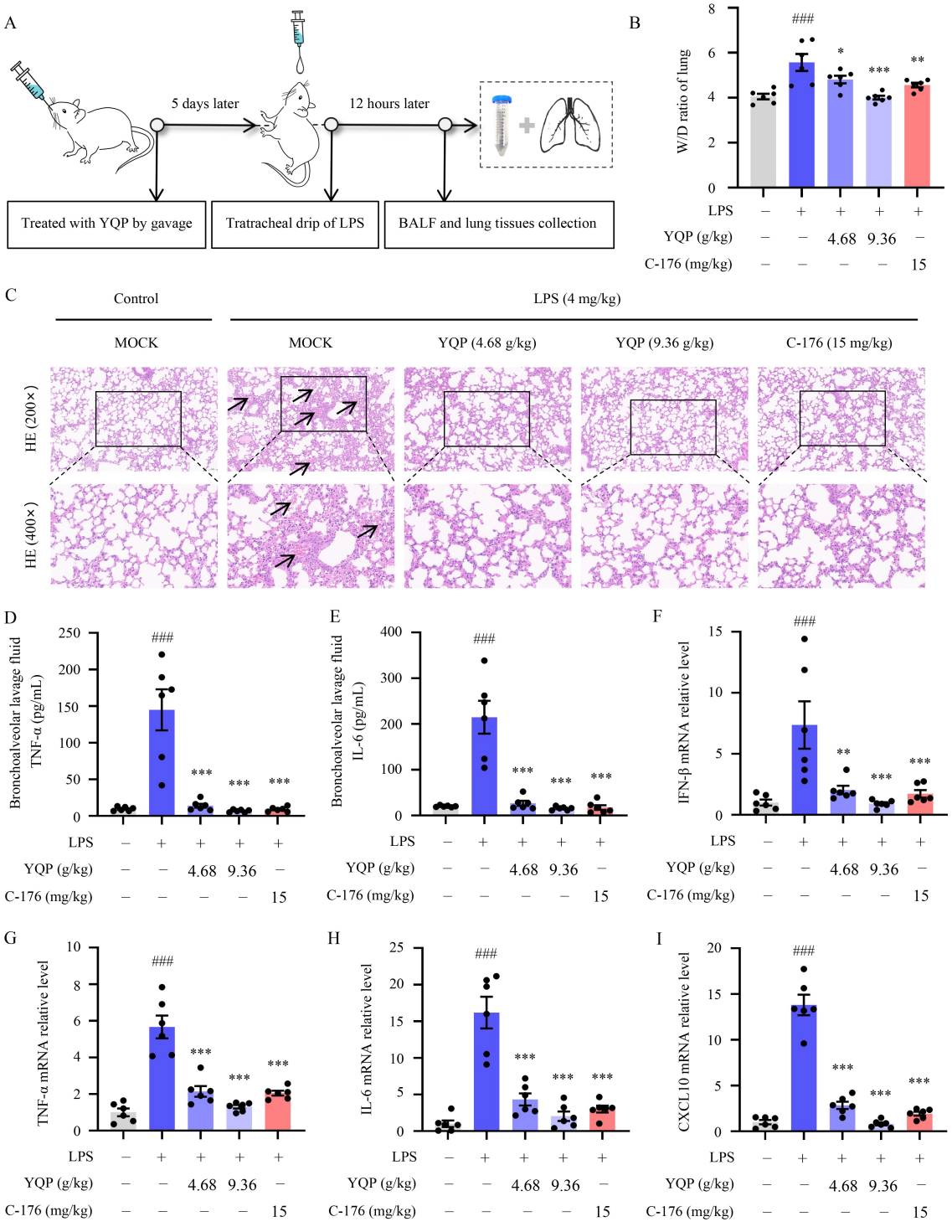

Fig. 5 YQP inhibits LPS-induced ALI in mice. (A) Schematic diagram of ALI mouse model and treatment process. (B) The W/D ratio of lung tissues. (C) Representative images of HE staining of lung tissues. (D–E) The expression levels of TNF-α and IL-6 in BALF were determined by ELISA. (F–I) The expression levels of IFN-β, TNF-α, IL-6 and CXCL10 in lung tissues were detected by qPCR. All data are expressed as mean ± SEM. Statistical differences were analyzed by one-way ANOVA and Dunnett's post hoc test. $^{###}P < 0.001$ vs. control group; $^{*}P < 0.05$, $^{**}P < 0.01$, $^{***}P < 0.001$ vs. model group.

morphology of the lung tissue was observed by HE staining. The lung tissues of mice developed obvious lesions after LPS administration, which mainly manifested as alveolar wall thickening, a significant increase in inflammatory cells, and obvious epithelial cell necrosis. As expected, treatment with different concentrations of YQP or C-176 improved the extent of lung injury with a gradual decrease in inflammatory cell infiltration (Fig. 5C). We also examined the levels of proinflammatory factors in the BALF. It proved that LPS enhanced the levels of TNF-α and IL-6 in BALF, whereas YQP and C-176 effectively reduced LPS-induced TNF-α and IL-6 expression (Fig. 5D and 5E). To further validate our findings, we examined the transcript levels of interferon-related genes (IFN-β and CXCL10) and proinflammatory factors (TNF-α and IL-6) in the lung tissues. These studies showed that the mRNA levels of these genes in the YQP groups were reduced in the lung tissues compared to those in the model group (Fig. 5F–5I). In summary, YQP effectively ameliorates LPS-induced ALI by suppressing the cGAS-STING pathway.

Discussion

ALI is a common respiratory emergency. Its pathogenesis is complex, and it has a high mortality rate [1]. Patients with ALI or ARDS have a mortality rate of more than 40% worldwide [48,49]. Although experts and scholars have been constantly improving and updating treatment strategies for ALI, safer and more effective treatments have not been found [45]. The cGAS-STING pathway is one of the crucial effect pathways of the body's natural immune system [50]. Recent studies have shown that it is linked to the initiation and development of many inflammatory diseases [51], including acute kidney failure [52], hepatitis B virus infection [53], and systemic lupus erythematosus [54]. Notably, it was recently shown that cGAS-STING participates in the regulation of inflammatory pulmonary injury. Therefore, the search for signaling modulators targeting the cGAS-STING pathway provides a promising disease direction for ALI treatment. YQP is a TCM compound that has been extensively used in clinical practice and has a variety of pharmacological activities, such as anti-inflammatory, anti-bacterial and anti-viral activities [31]. Here, we found that YQP effectively inhibited cGAS-STING pathway activation, thereby suppressing the expression of type I interferon and inflammatory cytokines both *in vitro* and *in vivo*. Meanwhile, YQP exhibited significant protective effects against lung injury in an LPS-induced ALI model, indicating that YQP could be an effective agent for the treatment of cGAS-STING-mediated ALI.

Here, we demonstrate that YQP can effectively inhibit the activation of the cGAS-STING signaling pathway and reduce levels of phosphorylated IRF3 and type I interferon. Furthermore, activated STING also modulated the NF-κB pathway and suppressed the expression of inflammatory cytokines. Importantly, we discovered that YQP did not affect STING oligomerization and speculated that it might target its effect after STING undergoes translocation. In further experiments, we investigated the interaction of YQP with proteins by transfecting exogenous plasmids and found that YQP could effectively inhibit the binding of TBK1-IRF3, but had no impact on STING-IRF3 or STING-TBK1. As indicated in previous studies, activated STING undergoes translocation from the endoplasmic reticulum to the Golgi apparatus during the recruitment and phosphorylation of TBK1 to form a complex, and TBK1 further phosphorylates STING. This complex further recruits IRF3 to form a functional STING signalosome, leading to IRF3 dimerization and nuclear entry to regulate type I interferon expression [14]. In our research, we discovered that YQP suppressed activation of the cGAS-STING pathway by blocking the binding of TBK1 to IRF3. In addition, we tried to explore the function of YQP on the cGAS-STING pathway activation at the *in vivo* level. It was reported that DMXAA is an exclusive STING agonist [55]. We injected DMXAA intraperitoneally after YQP treatment and detected the inflammatory response in the serum and intraperitoneal resident immune cells (monocytes and macrophages) in mice. As expected, YQP was effective in reducing the levels of type I interferon and inflammatory factors in the serum and peritoneal lavage fluid, which also proved our conclusion at the *in vivo* level.

ALI is an acute inflammatory process characterized by acute diffuse alveolar wall damage due to a variety of causes [56]. ALI occurs when lung cells are frequently exposed to external infections or other stimuli that result in cell damage or the release of pathogen DNA. These stimuli activate pattern recognition receptors present in the cytoplasm, which in turn promote cGAS-STING pathway activation. TNF-α and IL-6 are important proinflammatory factors, and their overexpression is a key factor to aggravate the degree of the inflammatory response [57]. Reducing the levels of pro-inflammatory factors helps alleviate the inflammatory response and is the basis for inflammatory diseases treating [58]. In our study, we found that intratracheal administration of LPS induces a marked inflammatory response in mice, leading to marked upregulation of key downstream molecules in the STING pathway. This aligns with previous literature reports indicating hyperactivation of cGAS-STING pathway under inflammatory conditions, confirming its involvement in the pathological progression of ALI. However, YQP not only suppressed type I interferon expression in the ALI mouse model but also reduced the levels of inflammatory cytokines. Both *in vivo* and

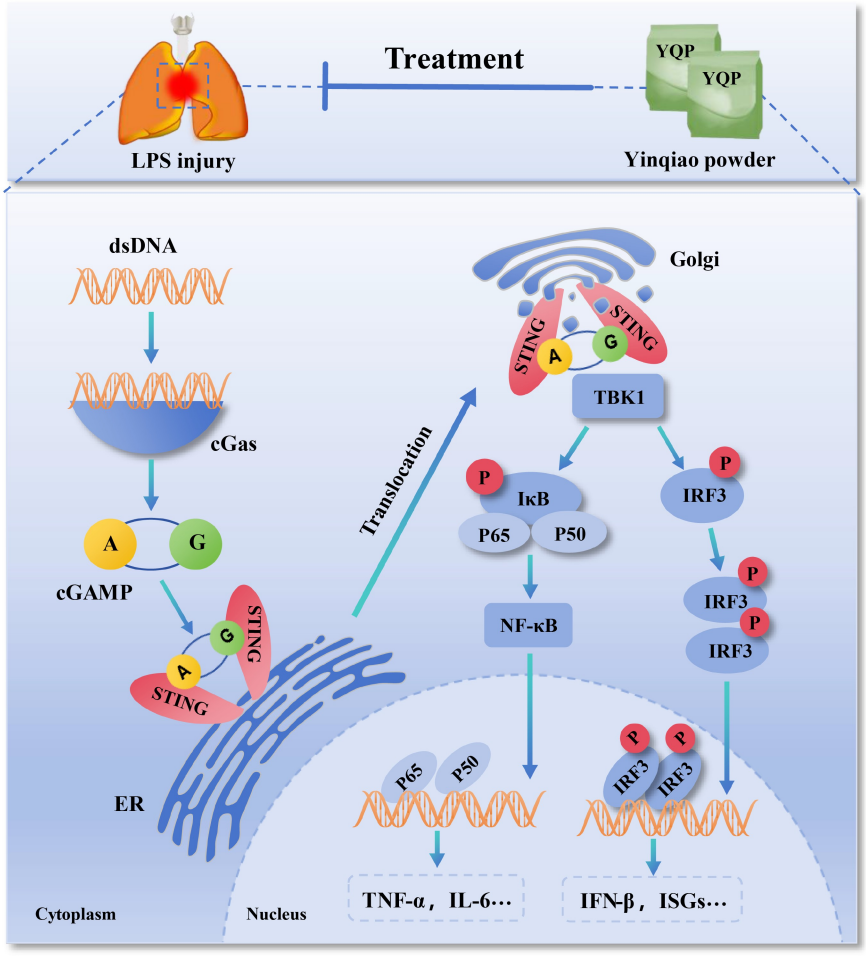

Fig. 6 YQP effectively inhibited the cGAS-STING pathway, suppressing the expression of type I interferons and inflammatory cytokines. YQP demonstrated a significant protective effect on ALI in mice induced by LPS.

in vitro experiments suggest that YQP effectively alleviates lung injury in mice by inhibiting the excessive activation of the cGAS-STING signaling pathway and suppressing inflammatory responses.

In conclusion, we have discovered a TCM compound, Yinqiao powder, which is effective in reducing the level of inflammation and improving the degree of lung injury in ALI mice and may be involved in inhibiting the cGAS-STING signaling pathway (Fig. 6). The study suggests that YQP may be a safe and effective modulator of the cGAS-STING pathway, which has a good potential to treat inflammatory diseases mediated by the cGAS-STING pathway.

Acknowledgements

This study was funded by the project of Cultivating and Improving the Service Ability of Traditional Chinese Medicine (No. 2021ZY038), National Natural Science Foundation of China (No. 82474095), General Hospital 3+1 Innovative Talent Construction Project.

Compliance with ethics guidelines

Conflicts of interest Hui Li, Jincai Wen, Yuanyuan Cui, Sichen Wang, Wei Shi, Huijie Yang, Li Lin, Yuanyuan Guo, Xiaohe Xiao, Junling Cao, Zhaofang Bai, and Ping Zhang declare that they have no known competing financial interests or personal relationships that could have appeared to influence the work reported in this paper.

All institutional and national guidelines for the care and use of laboratory animals were followed. Animal experiments were approved by the Laboratory Animal Welfare and Ethics Committee of the Fifth Medical Center of PLA General Hospital. The ethical approval number is IACUC-2021-0011.

Data availability and compliance statement

The authors declare that the acquisition and subsequent use of all data presented in this manuscript comply fully with all relevant local, national, and international laws, regulations, ethical guidelines, and the terms of use associated with the original data sources.

The authors bear full legal responsibility for ensuring the legality of data acquisition and all subsequent uses.

The original contributions presented in the study are included in the article. Further inquiries can be directed to the corresponding authors.

References

1. Butt Y, Kurdowska A, Allen TC. Acute lung injury: a clinical and molecular review. Arch Pathol Lab Med 2016; 140(4): 345–350
2. Mowery NT, Terzian WTH, Nelson AC. Acute lung injury. Curr Probl Surg 2020; 57(5): 100777
3. Devaney J, Contreras M, Laffey JG. Clinical review: gene-based therapies for ALI/ARDS: where are we now? Crit Care 2011; 15(3): 224.
4. Rao H, Song X, Lei J, Lu P, Zhao G, Kang X, Zhang D, Zhang T, Ren Y, Peng C, Li Y, Pei J, Cao Z. Ibrutinib prevents acute lung injury via multi-targeting btk, flt3 and egfr in mice. Int J Mol Sci 2022; 23(21): 13478
5. Zhang L, Li B, Zhang D, Zhao Y, Yu Q. lncRNA SNHG12 inhibition based on microsystem cell imaging technology protects the endothelium from LPS-induced inflammation by inhibiting the expression of miR-140-3p target gene fndc5. Contrast Media Mol Imaging 2022; 2022(1): 1681864
6. Li C, Liu JH, Su J, Lin WJ, Zhao JQ, Zhang ZH, Wu Q. LncRNA XIST knockdown alleviates LPS-induced acute lung injury by inactivation of XIST/miR-132-3p/MAPK14 pathway: XIST promotes ALI via miR-132–3p/MAPK14 axis. Mol Cell Biochem 2021; 476(12): 4217–4229
7. Janz DR, Ware LB. Biomarkers of ALI/ARDS: pathogenesis, discovery, and relevance to clinical trials. Semin Respir Crit Care Med 2013; 34(4): 537–548
8. Kellner M, Noonepalle S, Lu Q, Srivastava A, Zemskov E, Black SM. ROS signaling in the pathogenesis of acute lung injury (ALI) and acute respiratory distress syndrome (ARDS). Adv Exp Med Biol 2017; 967: 105–137
9. Wei J, Liu Z, Sun H, Xu L. Perillaldehyde ameliorates lipopolysaccharide-induced acute lung injury via suppressing the cGAS/STING signaling pathway. Int Immunopharmacol 2024; 130: 111641
10. Gao Z, Gao Z, Zhang H, Hou S, Zhou Y, Liu X. Targeting STING: from antiviral immunity to treat osteoporosis. Front Immunol 2023; 13: 1095577
11. Bai J, Liu F. The cGAS-cGAMP-STING pathway: a molecular link between immunity and metabolism. Diabetes 2019; 68(6): 1099–1108
12. Zhao J, Zhen N, Zhou Q, Lou J, Cui W, Zhang G, Tian B. NETs promote inflammatory injury by activating cGAS-STING pathway in acute lung injury. Int J Mol Sci 2023; 24(6): 5125
13. He YQ, Zhou CC, Deng JL, Wang L, Chen WS. Tanreqing inhibits LPS-induced acute lung injury *in vivo* and *in vitro* through downregulating STING signaling pathway. Front Pharmacol 2021; 12: 746964
14. Zhang X, Bai XC, Chen ZJ. Structures and mechanisms in the cGAS-STING innate immunity pathway. Immunity 2020; 53(1): 43–53
15. Ma R, Ortiz Serrano TP, Davis J, Prigge AD, Ridge KM. The cGAS-STING pathway: the role of self-DNA sensing in inflammatory lung disease. FASEB J 2020; 34(10): 13156–13170
16. Wang Y, Luo J, Alu A, Han X, Wei Y, Wei X. cGAS-STING pathway in cancer biotherapy. Mol Cancer 2020; 19(1): 136
17. Long ZJ, Wang JD, Xu JQ, Lei XX, Liu Q. cGAS/STING cross-talks with cell cycle and potentiates cancer immunotherapy. Mol Ther 2022; 30(3): 1006–1017
18. Zhuang X, Ma J, Xu G, Sun Z. SHP-1 knockdown suppresses mitochondrial biogenesis and aggravates mitochondria-dependent apoptosis induced by all trans retinal through the STING/AMPK pathways. Mol Med 2022; 28(1): 125
19. Chen C, Xu P. Cellular functions of cGAS-STING signaling. Trends Cell Biol 2023; 33(8): 630–648
20. Chen R, Du J, Zhu H, Ling Q. The role of cGAS-STING signalling in liver diseases. JHEP Rep Innov Hepatol 2021; 3(5): 100324
21. Pyclik M, Durslewicz J, Papinska JA, Deshmukh US, Bagavant H. STING agonist-induced skin inflammation is exacerbated with prior systemic innate immune activation. Int J Mol Sci 2023; 24(4): 4128
22. Hansen AL, Mukai K, Schopfer FJ, Taguchi T, Holm CK. STING palmitoylation as a therapeutic target. Cell Mol Immunol 2019; 16(3): 236–241
23. Jiang Z, Jiang Y, Fan J, Zhang J, Xu G, Fan Y, Zhang L, Qin X, Jiang X, Mao L, Liu G, Chen C, Zou Z. Inhibition of cGAS ameliorates acute lung injury triggered by zinc oxide nanoparticles. Toxicol Lett 2023; 373: 62–75
24. Huang YF, Li HY, Guo JX, Wang MX, Yang ZQ, Bai XY, Zhang ZD, Yang RY, Liu L, Zhou H, He F. Simultaneous determination of twenty-nine active compounds in fuzhengjiedu granules by HPLC-QQQ-MS/MS. Heliyon 2023; 9(2): e13675
25. Wang T, Lin S, Li H, Liu R, Liu Z, Xu H, Li Q, Bi K. A stepwise integrated multi-system to screen quality markers of Chinese classic prescription Qingzao Jiufei decoction on the treatment of acute lung injury by combining 'network pharmacology-metabolomics-PK/PD modeling'. Phytomedicine 2020; 78: 153313
26. Guo J, Zhu J, Wang Q, Wang J, Jia Y. Comparative efficacy of seven kinds of Chinese medicine injections in acute lung injury and acute respiratory distress syndrome: a network meta-analysis of randomized controlled trials. Front Pharmacol 2021; 12: 627751
27. Shu Y, Chen Y, Qin K, Liu X, Cai B. A study on the chemical compositions of the Yinqiaosan (*Lonicerae* and *Forsythiae* powder) at different time of later-decoction by gas chromatography mass spectrometry. Pharmacogn Mag 2016; 12(46): 134–138
28. Law AH, Yang CL, Lau AS, Chan GC. Antiviral effect of forsythoside A from *Forsythia suspensa* (Thunb.) Vahl fruit against influenza A virus through reduction of viral M1 protein. J Ethnopharmacol 2017; 209: 236–247
29. Fan Y, Liu W, Wan R, Du S, Wang A, Xie Q, Yang R. Efficacy and safety of yinqiao powder combined with western medicine in the treatment of pneumonia: a systematic review and meta-analysis. Complement Ther Clin Pract 2021; 42: 101297
30. Guo R, Zhao M, Liu H, Su R, Mao Q, Gong L, Cao X, Hao Y. Uncovering the pharmacological mechanisms of Xijiao Dihuang decoction combined with Yinqiao powder in treating influenza viral pneumonia by an integrative pharmacology strategy. Biomed Pharmacother 2021; 141: 111676
31. Zhang H, Xu L, Song J, Zhang A, Zhang X, Li Q, Qu X, Wang P. Establishment of quality evaluation method for Yinqiao powder: a herbal formula against COVID-19 in China. J Anal Methods Chem 2022; 2022(1): 1748324
32. Lin H, Wang X, Liu M, Huang M, Shen Z, Feng J, Yang H, Li Z, Gao J, Ye X. Exploring the treatment of COVID-19 with Yinqiao

powder based on network pharmacology. Phytother Res 2021; 35(5): 2651–2664
33. Deng D, Zhao M, Liu H, Zhou S, Liu H, You L, Hao Y. Xijiao Dihuang decoction combined with Yinqiao powder promotes autophagy-dependent ROS decrease to inhibit ROS/NLRP3/pyroptosis regulation axis in influenza virus infection. Phytomedicine 2024; 128: 155446
34. Fu YJ, Yan YQ, Qin HQ, Wu S, Shi SS, Zheng X, Wang PC, Chen XY, Tang XL, Jiang ZY. Effects of different principles of traditional Chinese medicine treatment on TLR7/NF-κB signaling pathway in influenza virus infected mice. Chin Med 2018; 13(1): 42
35. Li J, Dong M, Yao Q, Dong X, Chen Y, Wen J, Xu Y, Wu Z, Zhao X, Xiu Y, Zhan X, Bai Z, Xiao X. Amplifying protection against acute lung injury: targeting both inflammasome and cGAS-STING pathway by Lonicerae Japonicae Flos-Forsythiae Fructus drug pair. Chin Herb Med 2024; 16(3): 422–434
36. Wen J, Qin S, Li Y, Zhang P, Zhan X, Fang M, Shi C, Mu W, Kan W, Zhao J, Hui S, Hou M, Li H, Xiao X, Xu G, Bai Z. Flavonoids derived from licorice suppress LPS-induced acute lung injury in mice by inhibiting the cGAS-STING signaling pathway. Food Chem Toxicol 2023; 175: 113732
37. Ren L, Li Q, Li H, Zhan X, Yang R, Li Z, Fang Z, Liu T, Wei Z, Zhao J, Lin L, Mou W, Dai W, Bai Z, Xu G, Cao J. Polysaccharide extract from Isatidis Radix inhibits multiple inflammasomes activation and alleviate gouty arthritis. Phytother Res 2022; 36(8): 3295–3312
38. Conlon J, Burdette DL, Sharma S, Bhat N, Thompson M, Jiang Z, Rathinam VA, Monks B, Jin T, Xiao TS, Vogel SN, Vance RE, Fitzgerald KA. Mouse, but not human STING, binds and signals in response to the vascular disrupting agent 5, 6-dimethylxanthenone-4-acetic acid. J Immunol 2013; 190(10): 5216–5225
39. Chen Q, Sun L, Chen ZJ. Regulation and function of the cGAS-STING pathway of cytosolic DNA sensing. Nat Immunol 2016; 17(10): 1142–1149
40. de Oliveira Mann CC, Orzalli MH, King DS, Kagan JC, Lee ASY, Kranzusch PJ. Modular architecture of the STING C-terminal tail allows interferon and NF-κB signaling adaptation. Cell Rep 2019; 27(4): 1165–1175.e5
41. Wu Z, Lin Y, Liu LM, Hou YL, Qin WT, Zhang L, Jiang SH, Yang Q, Bai YR. Identification of cytosolic DNA sensor cGAS-STING as immune-related risk factor in renal carcinoma following pan-cancer analysis. J Immunol Res 2022; 2022: 7978042
42. Prabakaran T, Troldborg A, Kumpunya S, Alee I, Marinković E, Windross SJ, Nandakumar R, Narita R, Zhang BC, Carstensen M, Vejvisithsakul P, Marqvorsen MHS, Iversen MB, Holm CK, Østergaard LJ, Pedersen FS, Pisitkun T, Behrendt R, Pisitkun P, Paludan SR. A STING antagonist modulating the interaction with STIM1 blocks ER-to-Golgi trafficking and inhibits lupus pathology. EBioMedicine 2021; 66: 103314
43. Rocco PRM, Nieman GF. ARDS: what experimental models have taught us. Intensive Care Med 2016; 42(5): 806–810
44. Jiang K, Guo S, Yang C, Yang J, Chen Y, Shaukat A, Zhao G, Wu H, Deng G. Barbaloin protects against lipopolysaccharide (LPS)-induced acute lung injury by inhibiting the ROS-mediated PI3K/AKT/NF-κB pathway. Int Immunopharmacol 2018; 64: 140–150
45. Liu P, Hao J, Zhao J, Zou R, Han J, Tian J, Liu W, Wang H. Integrated network pharmacology and experimental validation approach to investigate the therapeutic effects of capsaicin on lipopolysaccharide-induced acute lung injury. Mediators Inflamm 2022; 2022: 9272896
46. Wu B, Xu MM, Fan C, Feng CL, Lu QK, Lu HM, Xiang CG, Bai F, Wang HY, Wu YW, Tang W. STING inhibitor ameliorates LPS-induced ALI by preventing vascular endothelial cells-mediated immune cells chemotaxis and adhesion. Acta Pharmacol Sin 2022; 43(8): 2055–2066
47. Li J, Liu L, Zhou X, Lu X, Liu X, Li G, Long J. Melatonin attenuates sepsis-induced acute lung injury through improvement of epithelial sodium channel-mediated alveolar fluid clearance via activation of SIRT1/SGK1/Nedd4-2 signaling pathway. Front Pharmacol 2020; 11: 590652
48. Sun X, Xiang H, Liu Z, Xiao H, Li X, Gong W, Pan L, Zhao L, Yao J, Sun C, Zhang G. Jingfang Granules alleviates bleomycin-induced acute lung injury through regulating PI3K/Akt/mTOR signaling pathway. J Ethnopharmacol 2024; 318(Pt A): 116946.
49. Shi CY, Yu CH, Yu WY, Ying HZ. Gut-lung microbiota in chronic pulmonary diseases: evolution, pathogenesis, and therapeutics. Can J Infect Dis Med Microbiol 2021; 2021: 9278441
50. Liu Z, Wang M, Wang X, Bu Q, Wang Q, Su W, Li L, Zhou H, Lu L. XBP1 deficiency promotes hepatocyte pyroptosis by impairing mitophagy to activate mtDNA-cGAS-STING signaling in macrophages during acute liver injury. Redox Biol 2022; 52: 102305
51. Zheng W, Xia N, Zhang J, Chen N, Meurens F, Liu Z, Zhu J. How the innate immune DNA sensing cGAS-STING pathway is involved in autophagy. Int J Mol Sci 2021; 22(24): 13232
52. Maekawa H, Inoue T, Ouchi H, Jao TM, Inoue R, Nishi H, Fujii R, Ishidate F, Tanaka T, Tanaka Y, Hirokawa N, Nangaku M, Inagi R. Mitochondrial damage causes inflammation via cGAS-STING signaling in acute kidney injury. Cell Rep 2019; 29(5): 1261–1273.e6
53. Zhao J, Xu G, Hou X, Mu W, Yang H, Shi W, Wen J, Liu T, Wu Z, Bai J, Zhang P, Wang Z, Xiao X, Zou W, Bai Z, Zhan X. Schisandrin C enhances cGAS-STING pathway activation and inhibits HBV replication. J Ethnopharmacol 2023; 311: 116427
54. Hagiwara AM, Moore RE, Wallace DJ, Ishimori M, Jefferies CA. Regulation of cGAS-STING pathway—implications for systemic lupus erythematosus. Rheumatol Immunol Res 2021; 2(3): 173–184
55. Liang J, Wang H, Ding W, Huang J, Zhou X, Wang H, Dong X, Li G, Chen E, Zhou F, Fan H, Xia J, Shen B, Cai D, Lan P, Jiang H, Ling J, Cheng Z, Liu X, Sun J. Nanoparticle-enhanced chemo-immunotherapy to trigger robust antitumor immunity. Sci Adv 2020; 6(35): eabc3646
56. Zhang V, Ganz T, Nemeth E, Kim A. Iron overload causes a mild and transient increase in acute lung injury. Physiol Rep 2020; 8(12): e14470
57. Jiang K, Yang J, Guo S, Zhao G, Wu H, Deng G. Peripheral circulating exosome-mediated delivery of miR-155 as a novel mechanism for acute lung inflammation. Mol Ther 2019; 27(10): 1758–1771
58. Chen L, Deng H, Cui H, Fang J, Zuo Z, Deng J, Li Y, Wang X, Zhao L. Inflammatory responses and inflammation-associated diseases in organs. Oncotarget 2018; 9(6): 7204–7218